FLOMEKO 2003
11th IMEKO TC9 Conference on Flow Measurement
Groningen, NETHERLANDS, 12 - 14 May 2003

INFLUENCE OF FLOW CONDITIONS ON AN ULTRASONIC FLOW METER

Olivier Broca, Joël Escande, Bruno Delenne, Gaz De France, Alfortville, France
Gérard Mouton, Gaz du Sud Ouest, Pau, France
Pierre Gajan, Alain Strzelecki, ONERA, Toulouse, France

Introduction

Multipath ultrasonic flow meters have been more and more used in gas industry for the last ten years, this technology represents an interesting alternative to orifice and turbine meters. In fact, ultrasonic meters offer significant advantages such as bi-directionality, low pressure loss, large range and self-checking capabilities. Nevertheless, in some specific configurations, ultrasonic meters are still sensitive to the installation conditions. During the last decade, this topic has been widely investigated on several aspects, however many questions still remain.

In Ultraflow project, Van Bloemendal et *al.*[1] and Vulovic et *al.*[2] examined the behaviour of multi-path flow meters located downstream of different pipe fittings, single bend, in or out of plan bends. Their study also focused on the influence of steps in the pipe diameter, the influence of the pressure and the flow meter orientation with respect to the upstream pipe configuration. Lunde et *al.*[3] performed similar measurements and completed their study with numerical simulations. The work performed at the Gas Research Institute by Grimley [4] combined flow metering error observations with velocity distribution measurements in the pipe. Hilgenstock et *al.*[5] applied CFD techniques in order to simulate installation effects on ultrasonic flow meters.

A detailed analysis of these works has been carried out, and the metering discrepancies obtained for a same pipe fittings have compared. We tried to determine the influence of different parameters such as the distance between the upstream fittings and the flow meter, the orientation of the flow meter or the pressure level. In most cases, the error decreases with the distance. The influence of the orientation is not obvious and depends on the flow characteristics at the flow meter location. Finally, this analysis indicates that the metering error is quasi-independent of the pressure line. Nevertheless, pressure drop had an influence on the signal to noise ratio and thus on metering error. The CFD techniques has given satisfactory results when applied to relative simple geometries like diffusers or contractions. For more complex geometries, the predictions becomes more hazardous.

Recently, ONERA has developed the ultrasonic tomography to correct the installation conditions influence on different kind of flow meters (Escande et *al.*[6] and Demolis et *al.*[7]). The new research program presented in this paper is financially supported by Gaz de France and Gaz du Sud Ouest.

Approach

To improve our knowledge about the ultrasonic flow meters behaviour, we need to provide a more detailed analysis of the relations between the flow conditions and the acoustic wave propagation. Based on conclusions of previous works, we develop the following strategy. In a first step, we described flow conditions downstream a header representative of an industrial gas installation to determine the amplitude of the induced flow perturbations. Thus, we could define an amplitude scale of elementary perturbations to study. We took into account two kinds of elementary perturbations : asymmetry and swirl. During these tests, we measured simultaneously the velocity profiles upstream of the sensors and the transit time of the ultrasonic wave.

In this paper, we analyse the influence of the ultrasonic path configuration and compare the deviations estimated from velocity profiles to the actual ones given by ultrasonic measurements.

Experimental set up

Tests are performed on an aerodynamic bench at ONERA Toulouse which works at the atmospheric pressure and for flow rates (Q) between 100 m^3/h and 1000 m^3/h. The reference meter is a turbine meter. The pipe diameter of the test section is 0.1 m (namely D). Velocity measurement downstream the header, i.e. a Te junction followed by a 90° elbow out of plan, are performed by both hot wire and laser Doppler anemometry. For elementary perturbations, we only use the hot wire anemometer for the flow characterisation. In each pipe section, four velocity profiles are performed each 45° (figure 1).

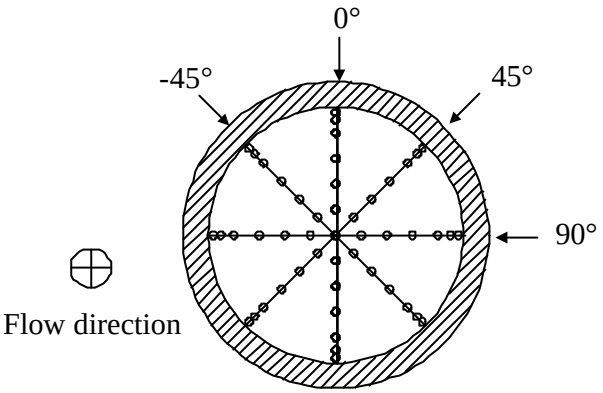

figure 1: Test section for velocity profile measurements; Investigated points are located by little circles

Elementary perturbations are generated with specific devices (Barbara and *al.*[8]). For asymmetric flow, we use an asymmetry generator based on a tube bundle system with tubes outlet shifted in the axial direction. The asymmetry level is qualified by a Td parameter defined as follows:

$$Td = 100 \cdot \left(\frac{Q_{r>0} - Q_{r<0}}{Q_{r>0} + Q_{r<0}} \right) \quad (1)$$

This parameter is expressed in percent and is calculates for each diameter. Thus, we determine the maximum intensity Td_{max} in the test section and its angular position.
Concerning swirling flow, we use a tangential flow generator, namely a swirler. The swirl angle is fixed by the ratio between tangential and total flow. It is defined as follows:

$$q_S = arctg\left(\frac{3S}{2}\right) \qquad \text{with} \qquad S = \frac{\int_0^R rU(rW)2\pi r dr}{R\int_0^R rU^2 2\pi r dr} \quad (2)$$

For difference transit time measurements, we use an industrial electronic unit developed by Panametrics®. This electronic controls the wave emission and reception and determines two transit times for each of two pairs of transducers. Two flow meter configurations are tested. Each of them is equipped with two pairs of ultrasonic transducers. The first meter is a two path arrangement, passing through pipe diameters. Acoustic paths make an angle of 45° with the pipe axis. One path is reflecting by the opposite wall. The second meter is formed by two chords placed in two parallel planes at two different radial positions. Here, the angle between acoustic paths and the pipe axis is 30°. A scheme describes these two acoustic configurations below (figure 2).

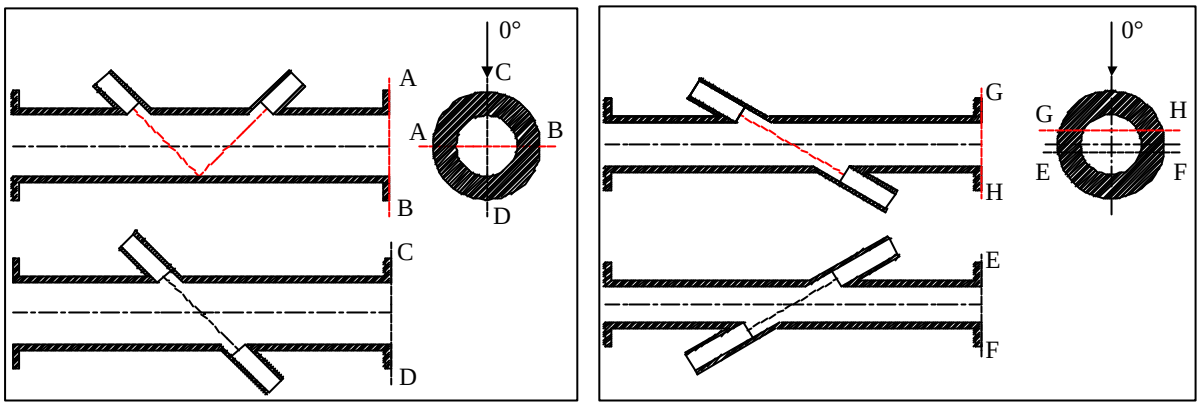

figure 2: On the left, meter 1 (Channel 1 on AB; Channel 2 on CD), and on the right, meter 2 (Channel 1 on EF, radial position 0.309R; Channel 2 on GH, 0.5R).

Tests carried out

The tests are performed for two flow rates (140 m^3/h and 280 m^3/h respectively) and different perturbations levels, in order to determine the relation between flow conditions and acoustic wave propagation. The rates considered corresponds to bulk velocities of 5 m/s and 10 m/s respectively. For asymmetry flows, we also check the influence of the meter orientation. On figure 2, section views represent meters in their position on bench at azimuthal position. Then, for meter 1, direct acoustic path (CD) is vertical at 0° and reflected acoustic path (AB) is horizontal for same angle. For meter 2, chords are horizontal at 0°, less off centre path (EF) is set on low part of the section, and the other one (GH) is in the upper part. The levels of perturbation for each flow rate are indicated in the following table:

140 m^3/h		280 m^3/h	
Td_{max} (%)	θ_S (°)	Td_{max} (%)	θ_S (°)
2.5	2	2.5	2
5	6	5	8
10	9	10	11
12.5	11	12.5	14
15	21	15	25

Table of elementary perturbation levels covered in this study

Data processing used

In the following section, we compare correction factor deviations measured on different ultrasonic paths with information determined from velocity profiles measured upstream of the flow meter. Transit time measurements allow us to determine an experimental correction factor (namely k_{US}) from the following expression:

$$k_{US} = \frac{U_0}{U_{lin.}} \quad (3)$$

U_0 is the mean velocity in the test section, and $U_{lin.}$ is the average flow velocity determined by ultrasonic transit time measurements and estimated as follows

$$U_{lin.} = \frac{c^2 \, \Delta t}{2L \cos q} \quad (4)$$

Where c is the velocity of sound in the test section, L the path length, Δt the difference transit time measured and θ the path angle with respect to the pipe axis.

We use the following expressions to determine a correction factor (namely k_{HW}) based on the velocity profile measured and a linear propagation model for the ultrasonic wave:

$$k_{HW} = \frac{U_0}{U_L} \quad (5)$$

$$U_0 = \frac{4}{p\,D^2}\int_0^{\frac{D}{2}} 2prU_x(r)dr \quad (6)$$

$$U_L = \frac{1}{L}\int_0^L \vec{U}\cdot\vec{t}\,dl \quad (7)$$

Where $\vec{t}$ is the unit vector tangent to the acoustic wave path, and U_x the axial velocity.

The velocity distribution along the acoustic path is determined from an interpolation of the measured velocity profiles.

Results and discussion

This section is divided in three parts. In the first part, we present some example of elementary perturbation flow obtained on the aerodynamic bench at the inlet of ultrasonic meter. Then, we present metering k deviations induced by these flow conditions. Finally, we present at first the numerical interpolation of velocity profiles measures along different chords, and we compare k deviations based on ultrasonic measurements with k deviations obtained from velocity profile measurements.

Velocity measurements

- Asymmetric flows

In figures 3 and 4, we plot the non dimensional velocity distribution measured 1D upstream of the flow meter with the generator of asymmetry. Each figure corresponds to a given flow rate, and three asymmetry levels.

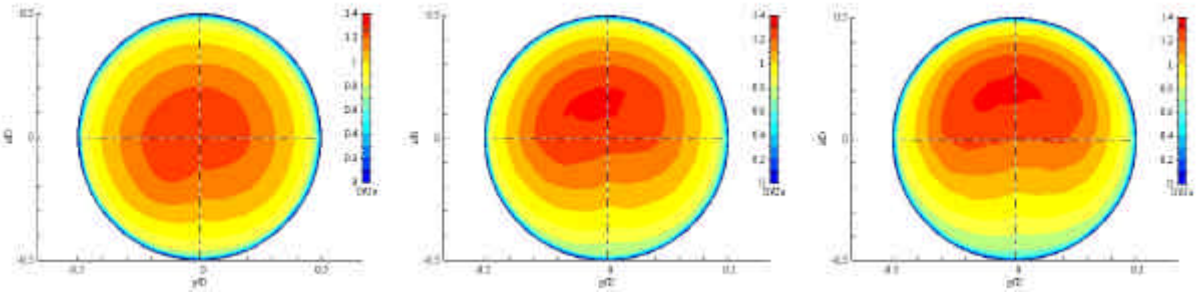

figure 3: Axial normalised velocity of asymmetric flows with Td=2.5%, 10% and 15% at 140m^3/h

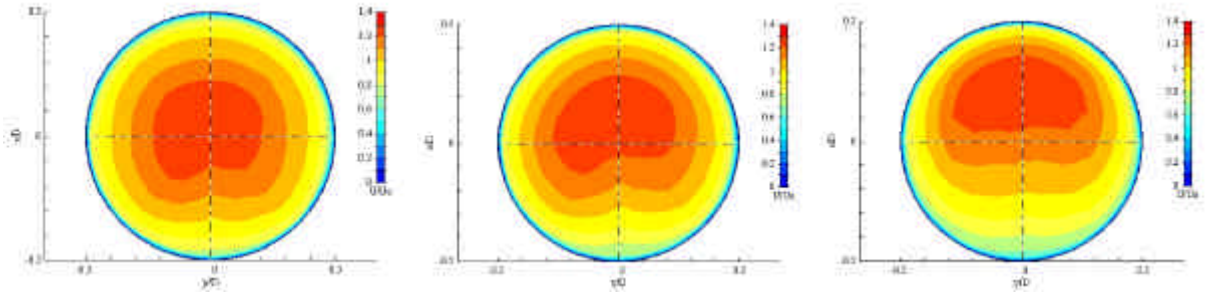

figure 4: Axial normalised velocity of asymmetric flows with Td=2.5%, 10% and 15% at 280m^3/h

On the figure above, we notice for the smaller value of Td a small perturbation on the axial flow compared to a fully developed turbulent flow. With an increased value of Td, we observe higher modifications on the axial velocity. The maximum of velocity is moving up in the test section. Here, the maximum of asymmetry is obtained on the vertical diameter which corresponds to an orientation of 0°. We observe that the axial velocity distribution is quite symmetrical in respect with the vertical diameter. Note that these flows are mainly axial, but flow is re-developed and the velocity has a radial component not accessible with our hot wire measurement system. A comparison between the mass flow rates obtained by velocity integration and the reference flow meter gave a shift lower than 1%.

- Swirling flows

We present the characterisation of the calibrated swirling flow in figures 5 to 8. In these figures, the non dimensional axial and tangential velocities are plotted versus non dimensional radial position.

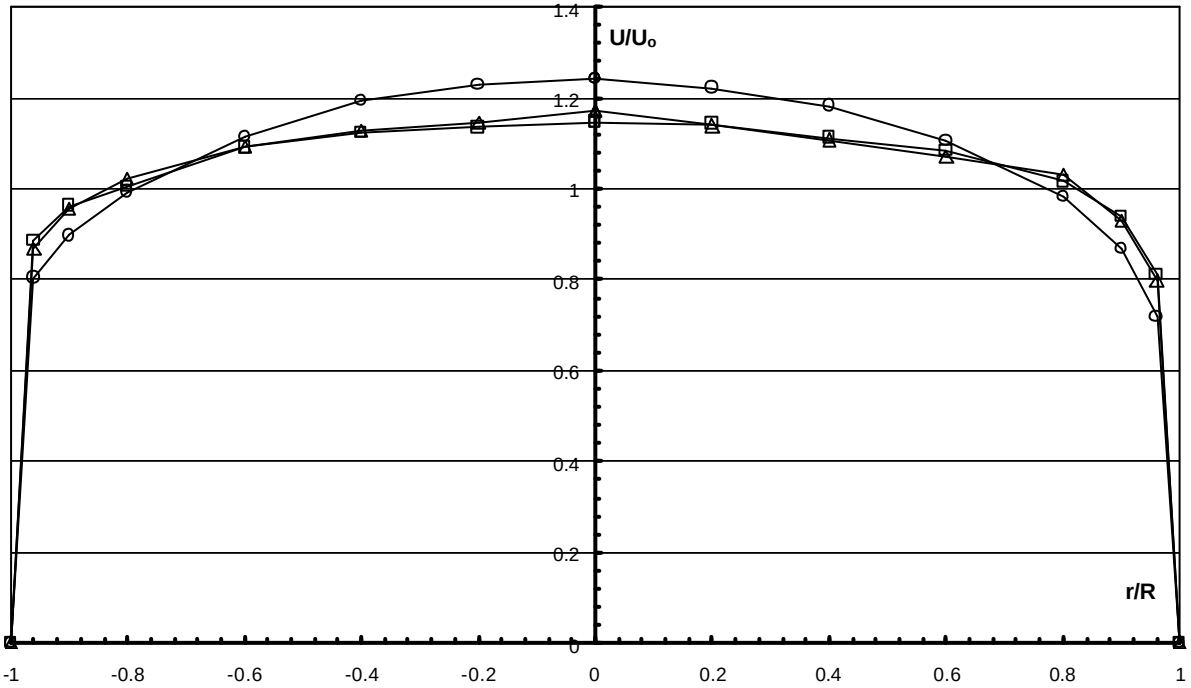

figure 5: Axial normalised velocity for flow rate 140 m^3/h; o for θ_S=2°; ÿ for θ_S=11°; Δ for θ_S=21°

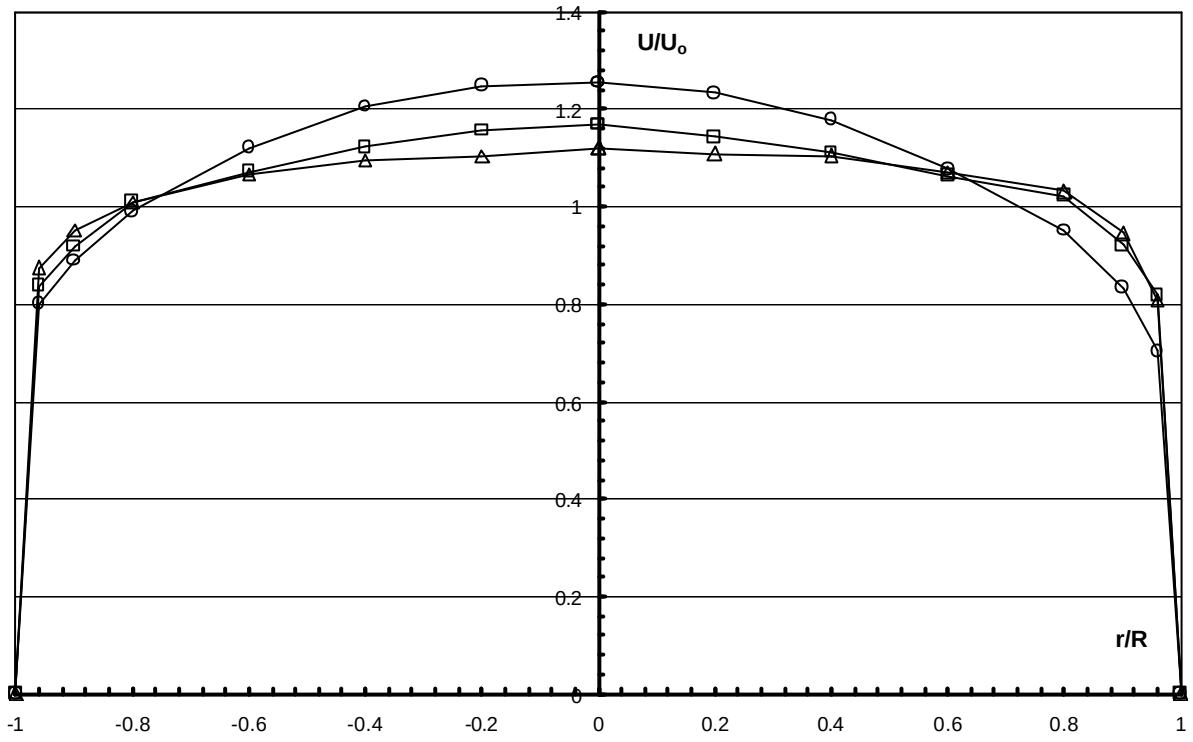

figure 6: Axial normalised velocity for flow rate 280 m^3/h; o for θ_S=2°; ÿ for θ_S=11°; Δ for θ_S=25°

The figures 5 and 6 show the axial component of the velocity for two flow rates and for three values of swirl angle. We notice that an increase of the swirl intensity flatten the velocity profile. For the lower flow rate, we observe that no evolution happens between the two higher swirl intensities. Nevertheless, between θ_S=11° and θ_S=21° for the flow rate 140 m^3/h, there is no variation on the axis velocity. The velocity profiles are well symmetric in relation to the pipe axis, except for the smallest swirl angle at higher flow rate.

In the figures 7 and 8, we represent the non dimensional tangential velocity. The velocity profiles are quite centred on the pipe axis at smaller flow rate, except for small swirl angle. For higher flow rate, the centre of rotation is slightly shifted out of the pipe axis. The deviation between the mass flow rate obtained from the velocity profile integration and the mass flow rate given by the reference meter increases. It can reach 5%.

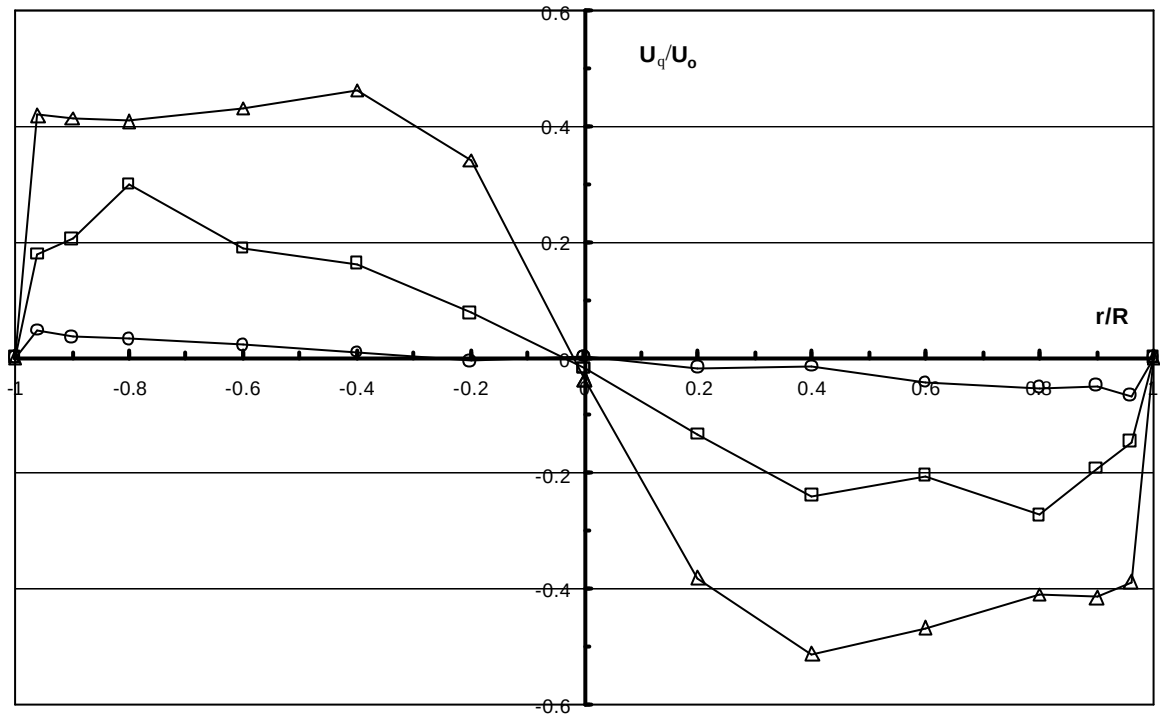

figure 7: Tangential normalised velocity for flow rate 140 m^3/h; ; o for $\theta_S=2°$; ÿ for $\theta_S=11°$; Δ for $\theta_S=21°$

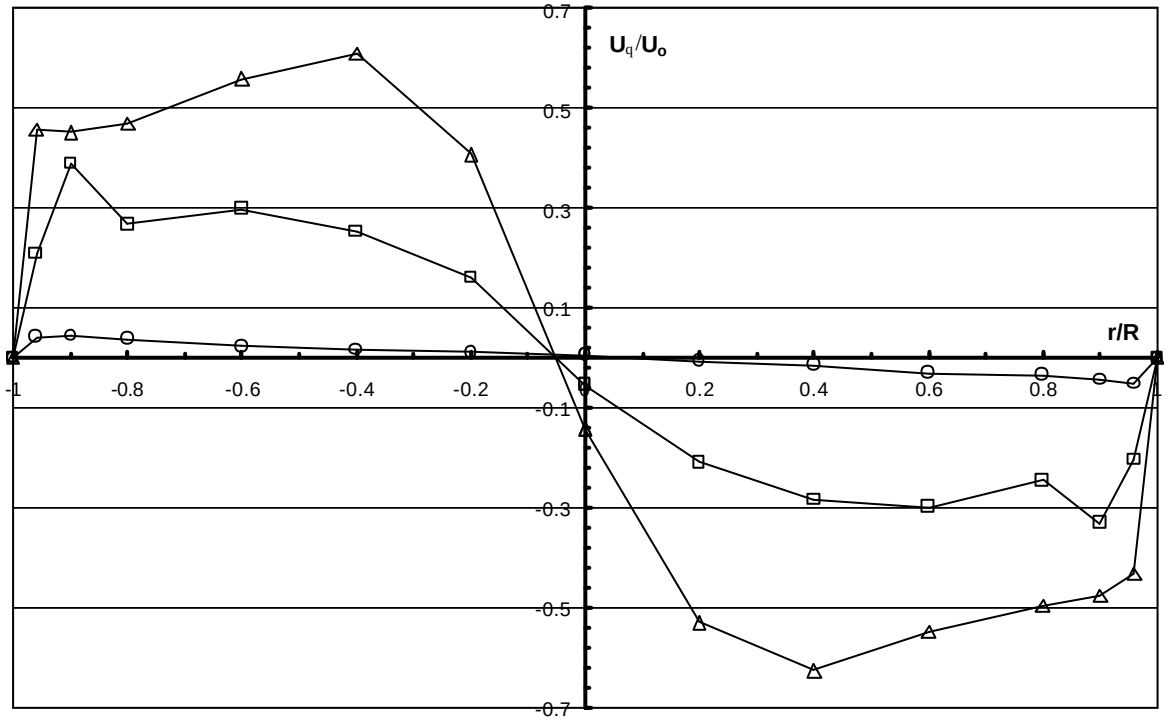

figure 8: Tangential normalised velocity for flow rate 280 m^3/h; ; o for $\theta_S=2°$; ÿ for $\theta_S=11°$; Δ for $\theta_S=25°$

Data analysis and discussion

For each elementary perturbed flow, we calculate k deviation, which represents the influence of flow conditions on the flow rate measurement. For each test, we present the k deviations on ultrasonic

measurement (namely E(US)) induced by elementary perturbations. These k deviations are calculated as follow:

$$E(US) = 100 \cdot \left(\frac{k_{US\,disturbed} - k_{US\,undisturbed}}{k_{US\,undisturbed}} \right) \quad (8)$$

The undisturbed value is obtained in fully developed flow conditions.

- Flow asymmetry

In this paper, we only present results for the conditions seen in figure 3 (Q_V=140 m^3/h). The k factors deviations with respect to the path orientation are plotted on figures 9 and 10. The distributions on figure 9 correspond to the path AB and CD for three values of parameter Td. The shape of the curves is periodic with the path orientation. The k factors deviations induced by the asymmetric perturbation lies between -2% and 4% (scale on vertical axis). The maximum errors due to asymmetry are obtained for orientations 90° and 270° for chord AB and at 0° and 180° for chord CD. In fact, for these orientations, the acoustic path followed the most asymmetric profile. An opposite tendency is observed for the path orientations 0° and 180°, and 90° and 270° for chords AB and CD respectively. For these orientations, profile velocity along the acoustic chords is almost symmetric. Nevertheless, it does not seem that parameter Td is bound with amplitude error. For example, we point out on the AB chord a deviation more important with Td=10% than with Td=15% for path orientation 270°. We observe that for two orientations spaced by 180°, we do not obtain equal ultrasonic k deviations. In a first step, we expected that this behaviour could be related to the influence of the cavities. An analysis of the obtained results for the lower flow rate accredits this hypothesis. This becomes less obvious with the results obtained with the higher flow rate.

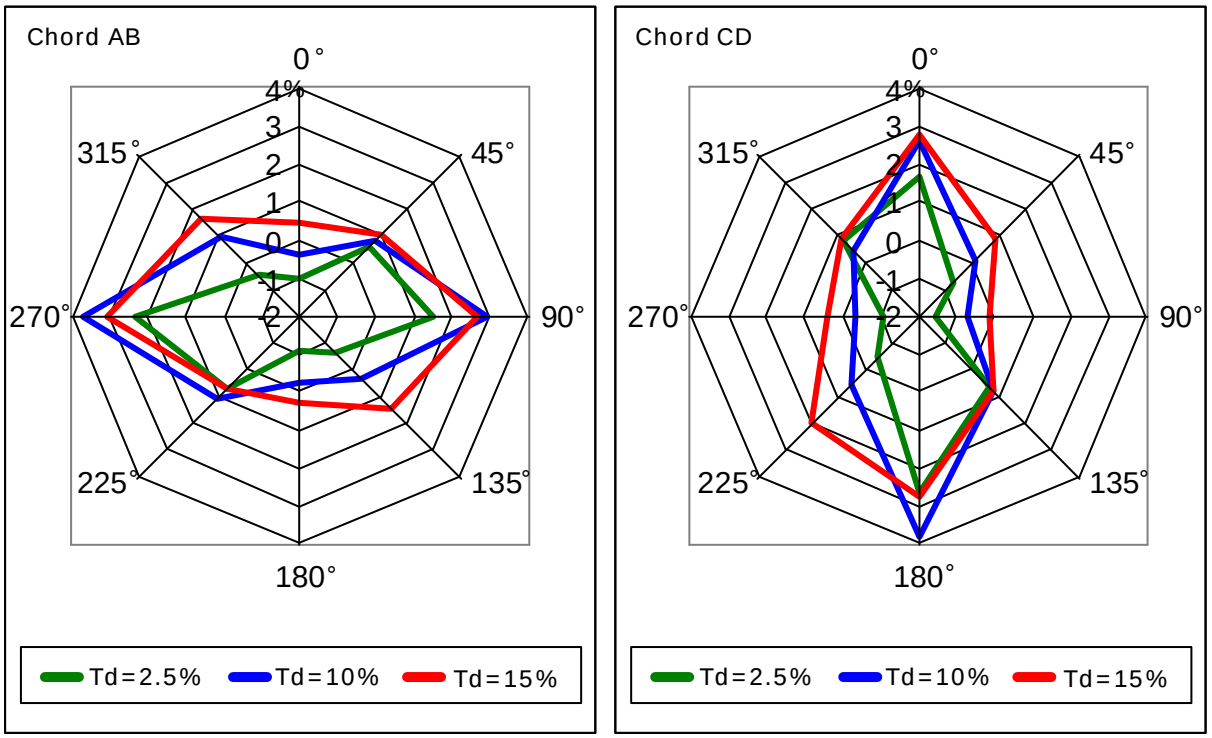

figure 9: k deviations obtained with different asymmetric flows versus path orientation on chord AB and CD

In figure 10, we present the k deviation obtained for the EF and GH chords of the meter 2. We note a periodic shape of this evolution as previously. Moreover, here the deviations on the k factors are more important than for centred chords. Metering k deviations are higher for EF chord than for GH chord that is more off centred.

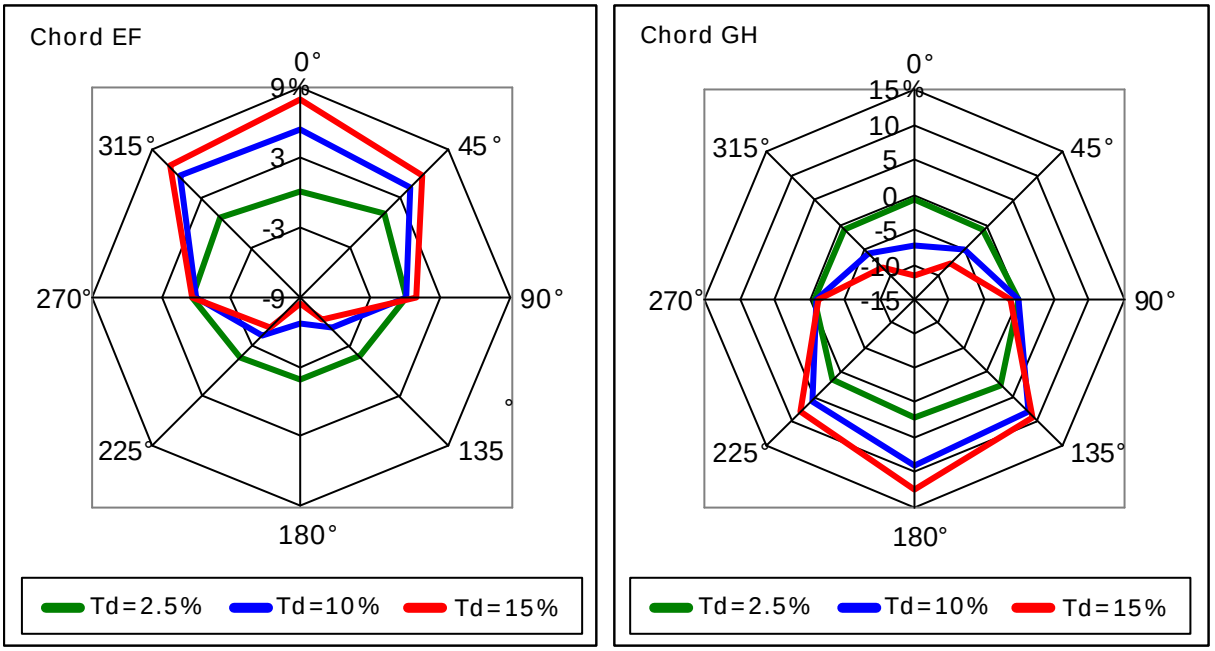

figure 10: k deviations obtained with different asymmetric flows versus path orientation on chord EF and GH

Above, the opposite sign obtained for extreme k deviation (for example at path orientation 0° and 180°) is explained by the position of chords relative to the maximum velocity in the test section. For 0° orientation, the maximum velocity is on the upper side of the test section, and the chord EF is located on the lower part of the test section. On this path the velocity distribution is always lower than the fully developed turbulent distribution. From relation (8), the error on the k factor is then positive. On the other hand, if the flow meter is oriented at 180°, velocity profile along the chord EF is higher and the error becomes negative. The behaviour of these paths indicates that it should be have a relation between the intensity of the perturbation and the metering error. The level of flow rate does not have a significant influence on the tested chords.

- Swirling flows

We present now k deviation factors obtained for a swirling flow with respect to the swirl intensity. In figure 11, we plot the results for the meter 1. This figure shows two areas. For low swirl intensity, the k deviations increases with the swirl intensity. Then it becomes quite constant. The limit between these two zones depends on the chords considered (6° for the chord AB and 10° for the chord CD). We note a similar k deviation behaviour in respect to the flow rate. Nevertheless, for low swirl angle (<2°), the k deviation is lightly higher for the lowest flow rate.

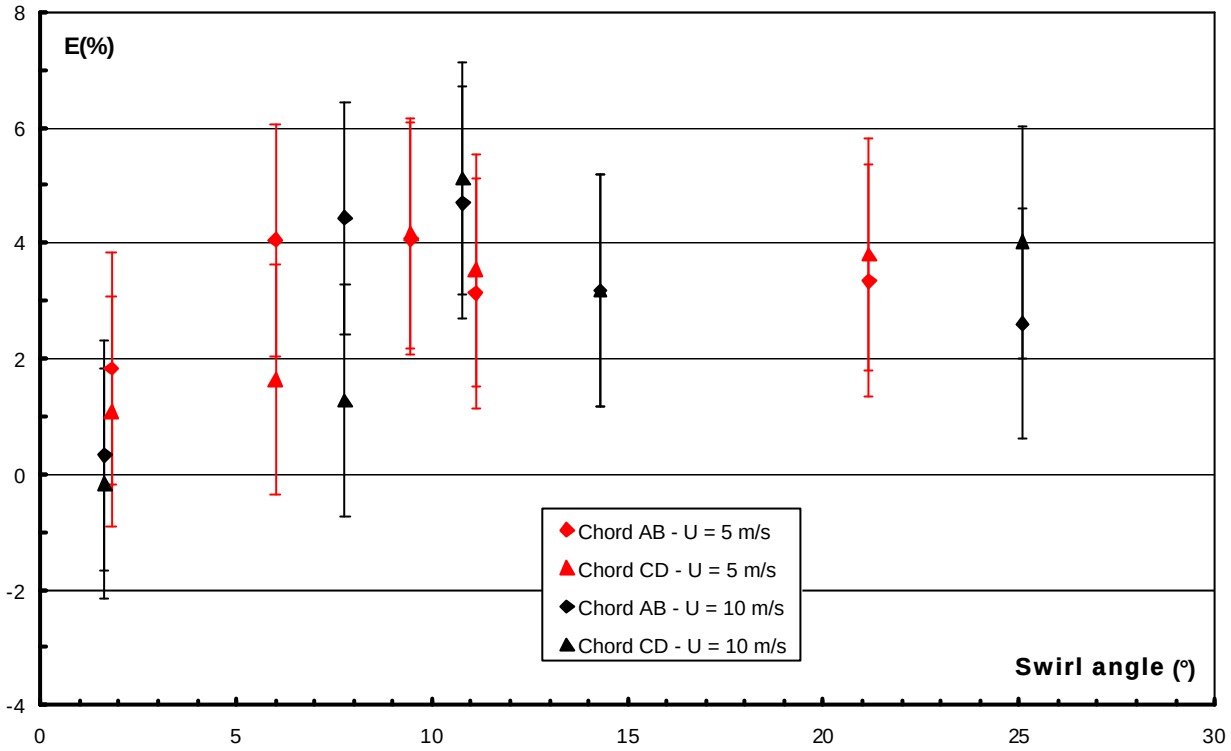

figure 11: k deviation versus swirl angle on chords AB and CD for two flow rates.

In figure 12, we present the same results for the meter 2. We notice that the influence of swirl angle is more important. This result can be related to the fact that ultrasonic paths are sensitive to the tangential velocity. We note a quite linear evolution of the error with respect to the swirl angle intensity. The metering error is more important for the lowest flow rate.

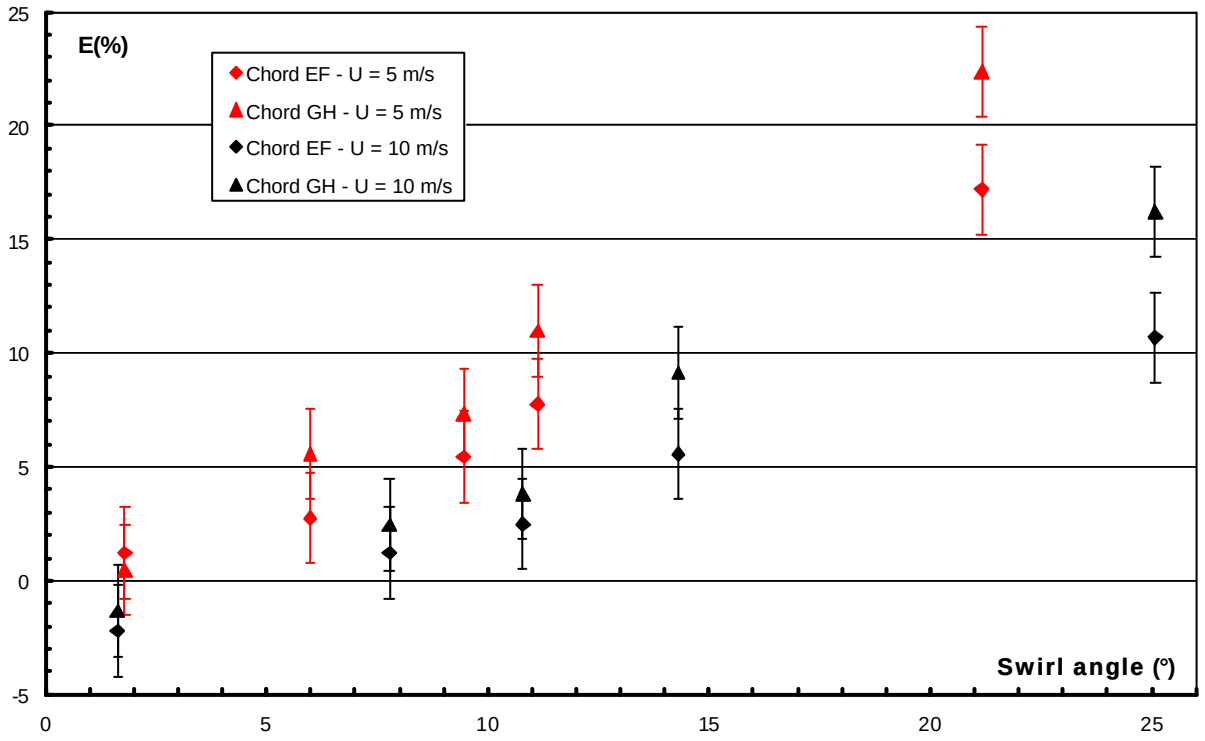

figure 12: k deviation versus swirl angle on chords EF and GH for two flow rates.

In the next part, we present comparisons between k deviations presented previously (ultrasonic measurements with and without perturbations) and calculations by a propagation model that accounts for velocity profiles measured in the pipe. Prior to these comparisons, we propose a validation of the numerical interpolation of velocity profiles along off centre chords.

- Validation of the interpolation method used to calculate the k_{HW} factor

Velocity profiles along four diameters spaced by 45° are measured. In order to determine the corrector factor k_{HW} (relation (5)), we have to interpolate these measurements. However, the interpolation procedure of the experimental results has to be validated. For that purpose, we use a theoretical expression of asymmetric flows proposed by Salami and *al.*[9]:

$$\frac{u(r,q)}{U_{max}} = \left(1-\frac{r}{R}\right)^{\frac{1}{n}} + m\frac{r}{R}\left(1-\frac{r}{R}\right)^{\frac{1}{k}} f(q) \qquad \text{with} \qquad f(q) = e^{(0.05p-0.2q)} \cdot \sin(q) \quad (9)$$

The first term of the second member of this relation is the Nikuradse relation for fully developed turbulent pipe flows. The second one accounts for radial distortion and angular variation through the function f(θ). We choose the values of the three constants n, m and k, to obtain an asymmetric flow representative of the perturbed flows measured on our bench. From the formula (9), it is possible to determine analytically the correction factor k on the acoustic paths of meter 2, and to simulate the "measured" velocity on the four diameters. Then, a bi-cubic interpolation of the profiles is performed on a refined mesh. This interpolation enables to determine the velocity distribution along the acoustic paths. In figures 13 and 14, we compare the interpolated distribution along acoustic paths with the exact solution (figure 13 for chord GH and figure 14 for EF chord).

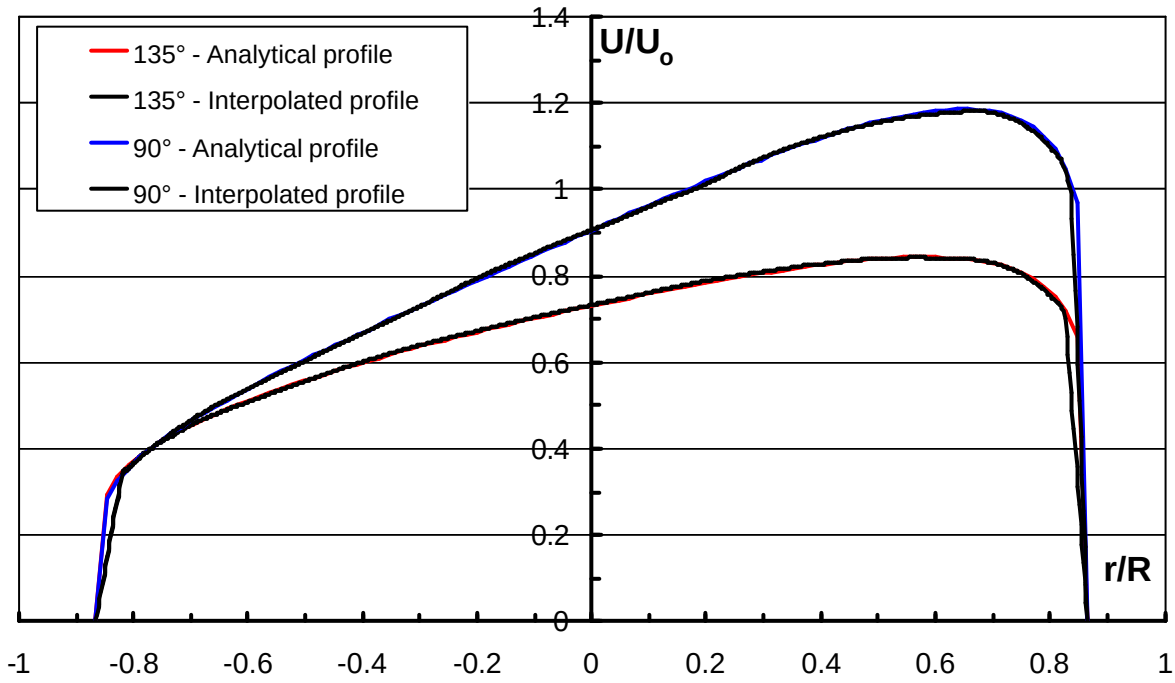

figure 13: Numerical reconstruction of a theoretical axial velocity profile along the chord GH (meter 2) for two orientations of it

On the figure above, we note a good agreement between theoretical profiles and numerical reconstruction. Nevertheless, we notice some discrepancies near the wall for a chord orientation of 90°. Therefore this behaviour is not observable with most of the asymmetric profile. We also notice few oscillations due to the bi cubic interpolation, notably in the region near the wall. On the following figure, we represent the same results for the EF chord (meter two).

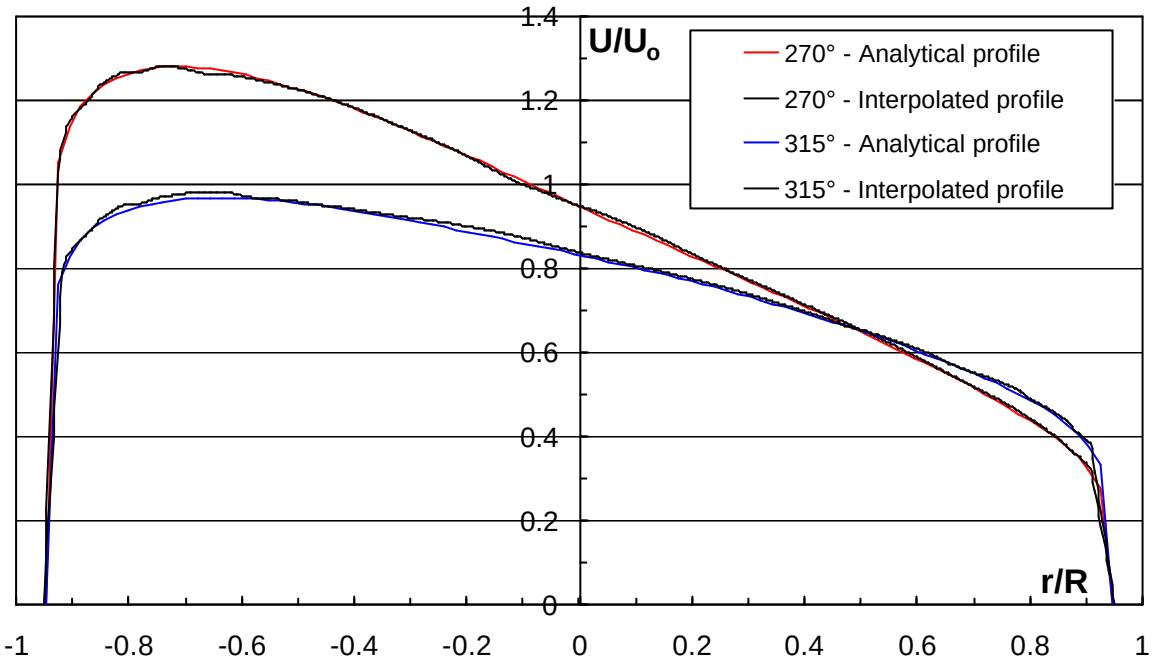

figure 14: Numerical reconstruction of a theoretical axial velocity profile along the chord EF (meter 2) for two orientations of it

This figure shows a good agreement between theoretical profiles and recalculated ones. The agreement near the wall for the lower asymmetry level is better here than in the previous ultrasonic path. We also observe some oscillations on the interpolate profile.
On the figure 15, we present interpolate profiles along these two chords for the measured asymmetric profile presented in figure 3.

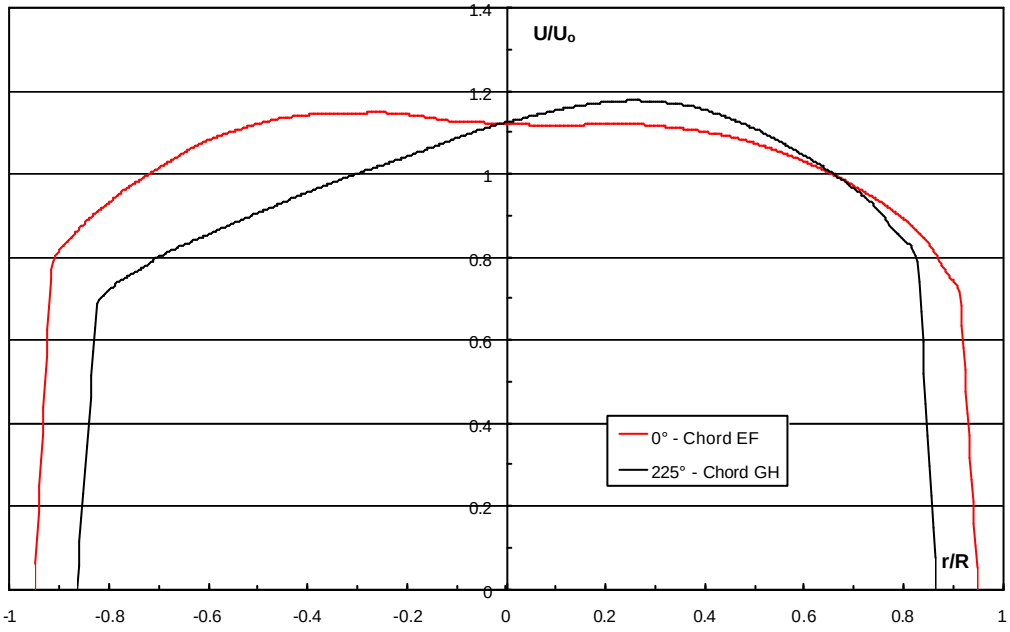

figure 15: Axial velocity profiles reconstruction from hot wire measurements for a flow rate 140 m^3/h and a Td=10%.

In this example, EF acoustic path is oriented at 0°. It means that this chord is horizontal on the lower side of the pipe (see figures 2 and 3). As a consequence, the red curve is rather symmetric. This numerical methods reproduces correctly the measured data. The GH chord is oriented at 225°. So, the interpolated profile is asymmetric. These numerical profile show few oscillations too.

Furthermore, if we compare the corrector factor obtained from the analytical expression with corrector factors calculated from velocity profile interpolation seen in figure 13 and 14, the difference is less than two percent (see the following figure 16).

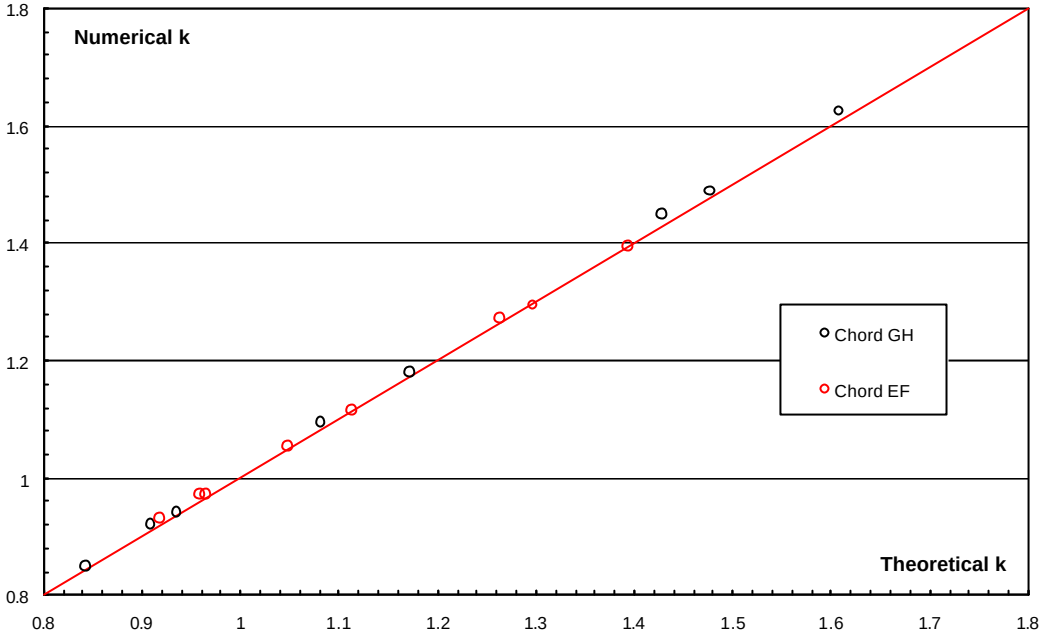

figure16: Comparison between numerical corrector factors with theoretical corrector factors for flow define by equation (9) and for eight orientations of chords equally spaced all around the test section.

Identical tests are carried out for a simulated swirling flow. The results give similar agreement between theoretical velocity profiles and interpolated one.

- Asymmetric flows

The k deviations obtained from velocity profiles and from difference transit time measurements with respect to path orientation are plotted on figures 17 and 18. K deviations from velocity profiles measurements are determined by the same relation (8), substituting k_{US} by k_{HW} to validate the ultrasonic meter behaviour model.

In figure 17, we present these results for two asymmetric flow. The shape of k deviations obtained from velocity profiles and from ultrasonic measurements are quite similar. Nevertheless, k deviations obtained from hot wire measurements tend to overestimate errors induced by asymmetric flow on this chords. The agreement deviations obtained from velocity profiles and from ultrasonic measurements is rather satisfying, less than 2%. We notice that error is between –2% and 4% (as in figure 9). There is no direct correlation between the k deviation and the level of the perturbation for meter one.

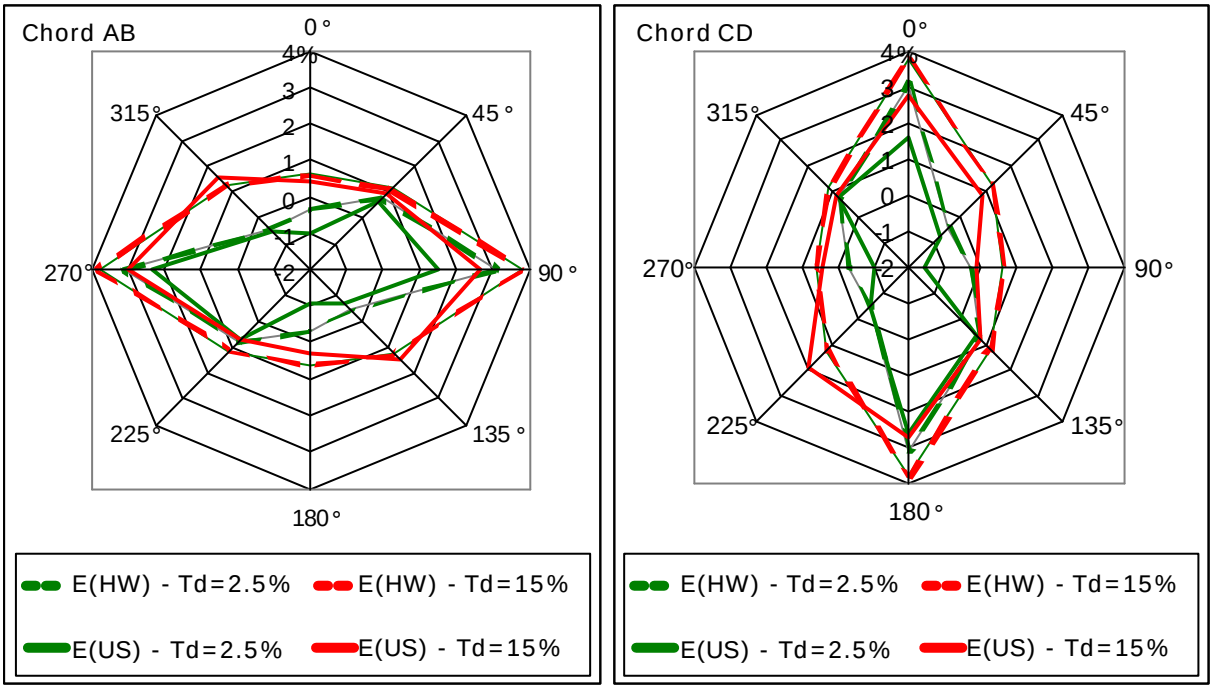

figure 17: k deviations due to asymmetric perturbation obtained from the model propagation E(HW) and from ultrasonic measurements E(US) for chords of meter 1 at 140 m^3/h versus path orientation

In figure 18, the same kind of representation is applied to the meter 2 on figure 18 The shape of k deviations in respect with path orientation is periodic, behaviour correctly reproduces by k deviations from velocity profiles. Nevertheless, we note a lesser agreement between k deviations from velocity profiles and from ultrasonic measurements than previously. As a matter of fact, as seen before the interpolation of the velocity profile induces an additional uncertainty which can reach in some cases 2%. Nevertheless a shift of 6% occurs on GH chord, for a path orientation 135°, and an asymmetry level of 10%.This might be due to a numerical interpolation error.

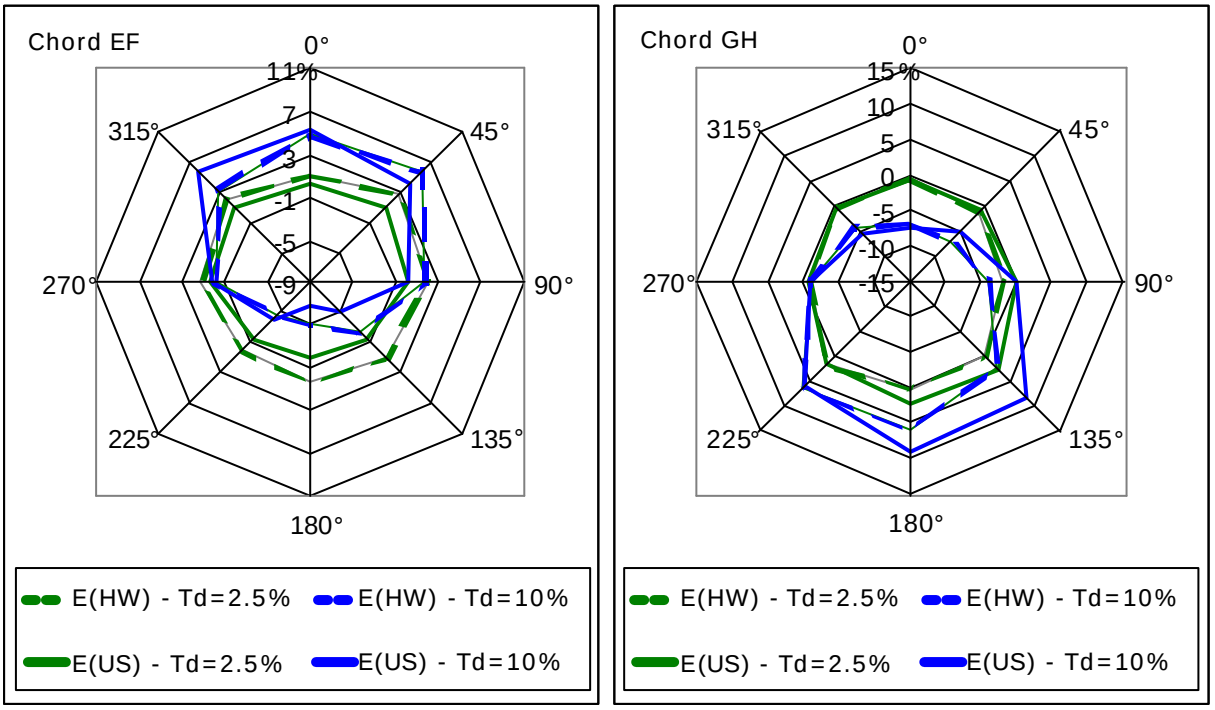

figure 18: k deviations due to asymmetric perturbation obtained from the propagation model E(HW) and from ultrasonic measurements E(US) for chords of meter 2 at 140 m^3/h versus path orientation

- Swirling flows

Comparison between k deviations factors computed from velocity profiles and ultrasonic measurements is done in figures 19 and 20. As before, the bisecting line corresponds to the ideal curve and the dotted ones to a shift of 1%. For all tests proposed, the agreement between k deviations obtained from the two ways is rather good.

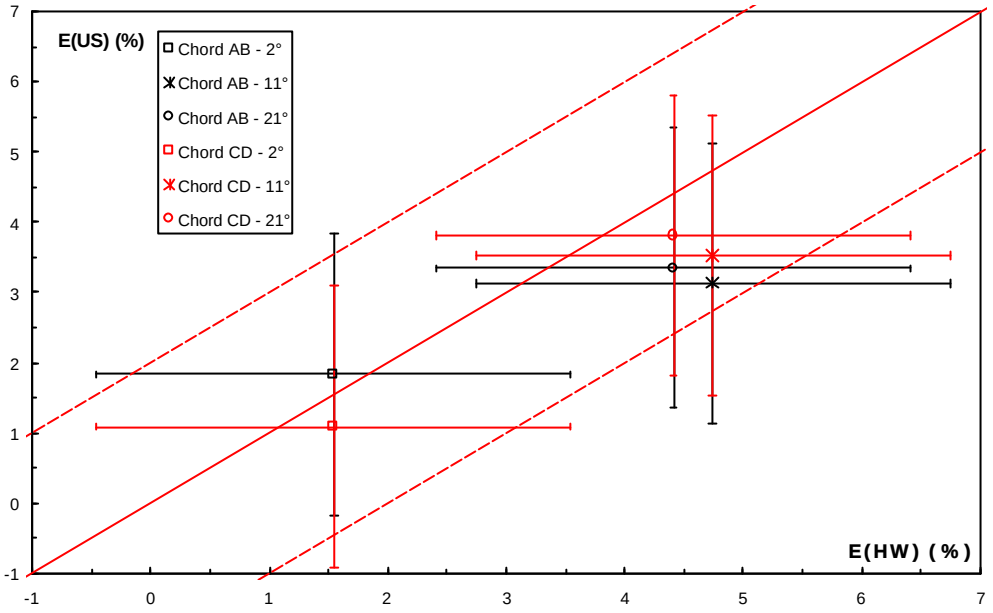

figure 19: Ultrasonic metering errors versus predicted errors using the propagation model for chords of meter 1 at 140 m^3/h for swirling flows conditions

We find again higher deviation level due to swirling flow on meter 2 with this two acoustic paths. The gap between k deviations obtained from velocity profiles measurements and ultrasonic measurements is more important for these two chords than for chords AB and CD. As seen previously, numerical interpolation induce an error lower than 2%. This additional error could explain the less agreement for chords CD and EF.

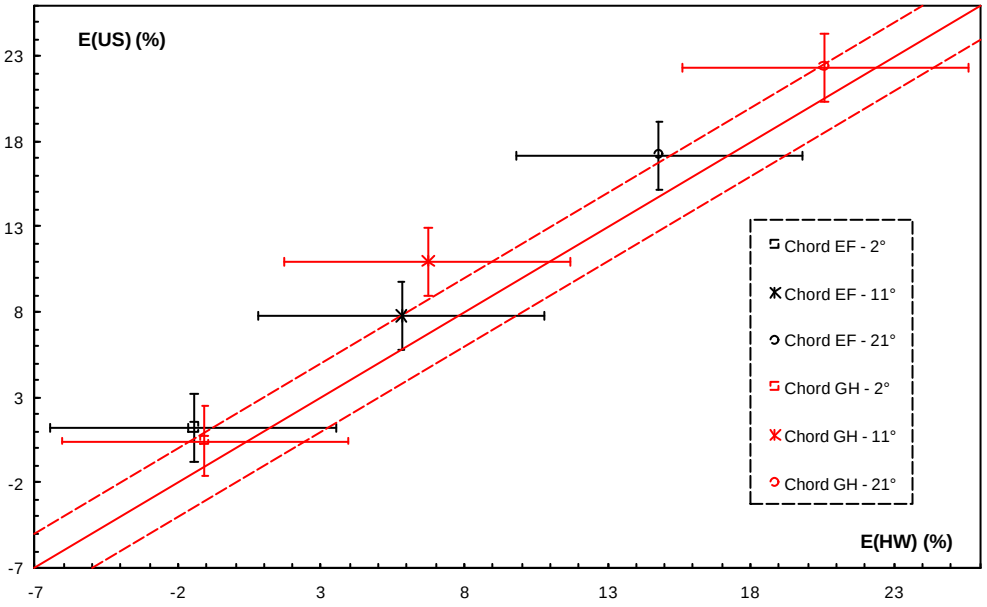

figure 20: Ultrasonic metering errors versus predicted errors using the propagation model for chords of meter 2 at 140 m^3/h for swirling flows conditions

Conclusions and prospects

This study focus on the influence of swirl and asymmetry on ultrasonic flow meters. Several level of each perturbations have been tested on four acoustic paths. Moreover the influence of acoustic path orientation was tested on asymmetric flow.

The k deviation induced by asymmetry on centred chords spreads between –2% and 4%, while the swirl may generate k deviation between –2% and 6%. The deviations observed on off centred chords are more important ; up to +/-14% for the most off centred chord when submitted to an asymmetric flow ; and between –5% and 25% with a swirling flow.
Two flow rates have been carried out. For each perturbed flow, except on off centre chords with swirling flow, the Reynolds number does not modify significantly the deviation. Contrary to off centred chords, the intensity of the flow perturbation does not affect the deviation for centred acoustic paths. Velocity profiles measurements enables to predict the ultrasonic deviation with acoustic path centred.

Optimisation of numerical interpolation of velocity profiles should enables to improve the predictions with other chords tested (meter 2). Some developments are still required to improve the propagation model and use it as a prediction tool. Along the same line, some more work is under way to evaluate the influence of calibrated pipe roughness on the time propagation of ultrasonic waves with respect to the velocity profile modifications.

References

[1] Installation effects on multi-path ultrasonic flow meters: The “Ultraflow” project, K. van Bloemendaal and P.M.A. van der Kam, North Sea Flow Measurement Workshop 1994

[2] Installation effects on a multi-path ultrasonic flow meter designed for profile disturbances, F. Vulovic, B. Harbrink and K. van Bloemendaal, North Sea Flow Measurement Workshop 1995

[3] Functional enhancements within ultrasonic gas flow measurement, P. Lunde, K.E. Froysa, J.B. Fossdal and T. Heistad, North Sea Flow Measurement Workshop 1999

[4] The influence of velocity profile on ultrasonic flow meter performance, T.A. Grimley, A.G.A. Operations Conference, 1998

[5] Numerical flow simulation as a tool for developing and calibrating ultrasonic flow meters, A. Hilgenstock, M. Heinz and B. Nath, Flomeko 1996

[6] 3D velocity profile reconstruction of gas flow in a pipe with ultrasonic tomography, Escande J., Gajan P. and Strzelecki A., Flomeko 2000

[7] The use of ultrasonic tomography to characterize internal flows in pipes, Demolis J., Escande J., Gajan P. and Strzelecki A., Flomeko 1998

[8] Experimental and numerical results on the flow through a 90° bend, Barbara O., Gajan P., Strzelecki A., De Laharpe V., Dutertre D. and Mouton G., Flomeko 1998

[9] Application of a computer to asymmetric flow measurement in circular pipes, L.A. Salami, Transactions Inst. M. C. vol. 6, n°4, 1984